

Efficacy and safety of the hypoxia-activated prodrug TH-302 in combination with gemcitabine and nab-paclitaxel in human tumor xenograft models of pancreatic cancer

Jessica D Sun*, Qian Liu, Dharmendra Ahluwalia, Wenwu Li, Fanying Meng, Yan Wang, Deepthi Bhupathi, Ayesha S Ruprell, and Charles P Hart

Threshold Pharmaceuticals; South San Francisco, CA USA

Keywords: gemcitabine, hypoxia-activated prodrug, hypoxia, nab-paclitaxel, pancreatic cancer, pharmacodynamics, biomarker, TH-302, xenograft

Abbreviations: T, TH-302; G, gemcitabine; nP, nab-paclitaxel; PDAC, pancreatic ductal adenocarcinoma; V, vehicle; EMT, epithelial to mesenchymal transition; Br-IPM, a brominated analog of isophosphoramidate mustard; BW, body weight; α -SMA, α smooth muscle actin; CAIX, carbonic anhydrase IX; CAF, cancer-associated fibroblast; MTD, maximum tolerated dose; NF, necrotic fraction; HF, hypoxic fraction; TGI, tumor growth inhibition; TGD₁₀₀₀, tumor growth delay compared to Vehicle reaching the size of 1000 mm³; CR, complete response; MT, median time to reach the size of 1000 mm³; ILS, increased life span.

Tumors often contain hypoxic regions resistant to chemo- and radiotherapy. TH-302 (T) is an investigational hypoxia-activated prodrug that selectively releases the DNA cross-linker bromo-isophosphoramidate mustard under hypoxic conditions. This study evaluated the efficacy and safety profile of combining T with gemcitabine (G) and nab-paclitaxel (nP) in human pancreatic ductal adenocarcinoma (PDAC) xenograft models in mice. Antitumor activity of the G + nP + T triplet was assessed and compared with T-alone or the G + nP doublet in the Hs766t, MIA PaCa-2, PANC-1, and BxPC-3 PDAC xenograft models. Efficacy was assessed by tumor growth kinetic analysis. Body weight, blood cell counts, blood chemistry, and the von Frey neuropathy assay were analyzed to evaluate safety profiles. Pharmacodynamic changes after the treatment were determined by immunohistochemistry of cell proliferation, DNA damage, apoptosis, hypoxia, and tumor stroma density. The G + nP + T triplet exhibited enhanced efficacy compared with T-alone or the G + nP doublet. Compared with vehicle (V), G + nP induced body weight loss, reduced neutrophil and lymphocyte counts, increased the levels of liver function parameters, and induced neurotoxicity. However, when T was added to G + nP, there was no statistically increased impairment compared to G + nP. The triplet significantly increased DNA damage, apoptosis, and tumor necrosis. Furthermore, the triplet further inhibited cell proliferation and reduced stroma density and intratumoral hypoxia. The triplet combination of G + nP + T exhibited superior efficacy but additive toxicity was not evident compared to the G + nP doublet in this study. This study provides a translational rationale for combining G, nP, and T in the clinical setting to assess efficacy and safety. A Phase I clinical trial of the triplet combination is currently underway (NCT02047500).

Introduction

Regions of tumor hypoxia, or low-oxygen conditions, are a common feature of the microenvironment of many solid tumors and hematological malignancies.^{1–4} Published studies show that the magnitude and extent of tumor hypoxia correlate directly with poor clinical prognosis.⁵ The basis for the correlation

between tumor hypoxia and prognosis has been ascribed to both therapeutic treatment failure and hypoxia-induced pro-metastatic potential.^{6–9} Hypoxia association with treatment failure is exhibited as resistance to radiotherapy and chemotherapy and the presence of quiescent hypoxic cells resistant to anti-proliferative therapy.⁵ The contribution of hypoxia to a more aggressive, invasive, and metastatic phenotype involves multiple mechanisms,

© Jessica D Sun, Qian Liu, Dharmendra Ahluwalia, Wenwu Li, Fanying Meng, Yan Wang, Deepthi Bhupathi, Ayesha S Ruprell, and Charles P Hart

*Correspondence to: Jessica D Sun; Email: jsun@thresholdpharm.com

Submitted: 10/21/2014; Revised: 12/20/2014; Accepted: 12/23/2014

<http://dx.doi.org/10.1080/15384047.2014.1003005>

This is an Open Access article distributed under the terms of the Creative Commons Attribution-Non-Commercial License (<http://creativecommons.org/licenses/by-nc/3.0/>), which permits unrestricted non-commercial use, distribution, and reproduction in any medium, provided the original work is properly cited. The moral rights of the named author(s) have been asserted.

including: promotion of genetic¹⁰ and epigenetic changes;¹¹ inhibition of apoptosis;¹² a shift to glycolytic metabolism;¹³ up-regulation of survival factors;¹⁴ production of enzymes mediating invasiveness;¹⁵ stimulation of angiogenic signals;¹⁵ induction of epithelial to mesenchymal transition (EMT);¹⁶ and preferential location of cancer stem cells to hypoxic subregions.¹⁷

TH-302 (1-Methyl-2-nitro-1*H*-imidazol-5-yl)methyl *N,N'*-bis(2-bromoethyl)phosphorodiamidate is a hypoxia-activated prodrug composed of 2-nitroimidazole linked to a brominated analog of isophosphoramidate mustard (Br-IPM).¹⁸ The 2-nitroimidazole moiety of TH-302 is a substrate for intracellular 1-electron reductases and, when TH-302 is reduced under hypoxic conditions, Br-IPM is released. TH-302 exhibits hypoxia-selective *in vitro* cytotoxicity across a wide variety of human cancer cell lines¹⁹ and *in vivo* anti-tumor efficacy in a panel of human tumor xenograft models.^{20,21}

Pancreatic ductal adenocarcinoma (PDAC) is one of the most aggressive tumors in humans, with a 5-year survival rate of less than 5%.²² Gemcitabine, a cytotoxic pyrimidine analog chemotherapeutic, has been the standard first-line treatment for patients with unresectable locally advanced or metastatic pancreatic cancer.²³ Gemcitabine-based chemotherapy doublets have been investigated in numerous Phase 2 and 3 trials. Until recently, these trials failed to show a statistically significant survival benefit except for the gemcitabine-erlotinib combination trial.²⁴ The addition of TH-302 to gemcitabine in a randomized Phase 2 PDAC clinical trial demonstrated a significant increase in progression-free survival compared with gemcitabine only (NCT01144455).²⁵ A Phase 3 trial of the gemcitabine and TH-302 combination compared to gemcitabine and placebo is currently underway (NCT01746979). Nab-paclitaxel is a human serum nanoparticle albumin-bound formulation of paclitaxel designed to overcome solubility problems associated with paclitaxel.²⁶ Recently gemcitabine in combination with nab-paclitaxel demonstrated a statistically significant survival benefit, and has been approved by FDA and EMA for 1st line treatment of metastatic pancreatic cancer.²⁷

Combination therapies that work on different molecular targets or different cellular compartments in the cancer process should in theory increase the probability of eliminating the cancer and decrease the likelihood of the development of resistant cancer cells. Gemcitabine is a normoxic compartment-selective conventional chemotherapeutic, and TH-302 is a hypoxia compartment-selective agent. Nab-paclitaxel has been shown to affect the tumor stroma.^{28,29} In the present study, we evaluated the efficacy and safety profile of TH-302 in combination with gemcitabine and nab-paclitaxel in PDAC preclinical models.

Results

Addition of TH-302 enhances the antitumor activity of gemcitabine and nab-paclitaxel

Hs766t, MIA PaCa-2, PANC-1, and BxPC-3 PDAC xenograft models were used to analyze the antitumor effect of the different treatment regimens. Groups of 10 animals were treated

with Vehicle (V), TH-302 (T) alone, the gemcitabine and nab-paclitaxel (G + nP) doublet, or the triplet of G + nP + T with the following doses and regimens: G, 60 mg/kg, ip, Q3Dx5; T, 50 mg/kg, ip, Q3Dx5; nP, 30 mg/kg, iv, Q3Dx5. When combination treatment was scheduled, T was given first, followed by nP 2 hrs later, and 1 hr after administration of nP, G was given. This preclinical dosing sequence is consistent with Phase 2 and Phase 3 clinical trial design of G and T combination (NCT01144455 and NCT01746979, respectively) as well as the administration of G and nP in PDAC patients approved by the FDA and EMA. 50 mg/kg of TH-302 employed in this study was equivalent in terms of resulting AUC to the doses being tested in the ongoing Phase 1 trial of TH-302 plus gemcitabine plus nab-paclitaxel in pancreatic cancer (NCT02047500). In this trial, TH-302 is administered at a dose ranging from 170–340 mg/m². This could be converted to 32–64 mg/kg in the tumor bearing mice, calculated by the pharmacokinetic data from the clinical studies and the mouse studies based on linear pharmacokinetics.^{30,31}

100 mg/kg T is considered as maximum tolerated dose (MTD) as a single agent and the dose of 50 mg/kg was 1/2 MTD. As a monotherapy at 50 mg/kg, T exhibits modest to moderate antitumor activity in the MIA PaCa-2, PANC-1, and BxPC-3 models, yielding TGIs of 27%, 45%, and 43% respectively (Fig. 1, and Table 1). In the Hs766t model, T monotherapy dramatically inhibited tumor growth, with a TGI of 82%.

The doublet of G + nP significantly inhibited tumor growth in all 4 models, exhibiting TGIs from 85% to 107%. When T was added to the doublet, the antitumor activity was increased. The TGI also increased in MIA PaCa-2 and PANC-1 models, to 120% and 110%, respectively, which was significantly increased compared with TH-302 monotherapy or G + nP doublet.

A Kaplan-Meier plot was used to calculate the median time (MT) to reach a tumor size of 1000 mm³ (Fig. 1 and Table 1). The triplet combination therapy treated group in the Hs766t model showed MT of 65 days, which was significantly prolonged compared with T monotherapy of 60 days or G + nP doublet combination therapy of 50 days. Similar results were also observed in the MIA PaCa-2, PANC-1, and BxPC-3 models: the G + nP doublet combination therapy demonstrated antitumor activity, and when T was added, the efficacy was enhanced. In all 4 models, the triplet combination therapy statistically increased the antitumor activity and prolonged survival compared with T monotherapy. A statistical difference by log-rank test between the triplet combination therapy group and the G + nP doublet combination therapy group was seen only in the H766t model.

In three of the 4 models, the triplet combination therapy increased the complete response (CR) rate relative to the G + nP combination therapy or T monotherapy (Table 1). Of note, the CR rate of the G + nP + T combination therapy in the PANC-1 model reached 100%, compared to 10% and 60% in the T monotherapy and G + nP combination therapy groups, respectively. In the MIA PaCa-2 model, the CR rate in the triplet group was 90%, compared to 0 and 30% in the T monotherapy and G + nP doublet combination therapy groups, respectively (Table 1).

In the Hs766t and MIA PaCa-2 models, approximately 10 days after the last treatment, a further tumor growth regression in the treatment groups, particularly in G+ nP + T group, was observed. Similar results have been consistently seen in previous studies. We performed an experiment to compare morphology of vehicle and G + nP + T treated tumors at a similar size in Hs766t xenograft tumors. Hs766t xenograft exhibited morphology of a cystic tumor. Fluid filled the cystic space by gross pathology. After G + nP + T treatment, the majority of the tumor exhibited a necrotic phenotype, manifested as a viable rim with a large necrotic core. As the fluid was gradually absorbed over time, the tumor size shrank further (Fig. S1).

No additional toxicity observed on adding TH-302 to gemcitabine and nab-paclitaxel as assessed by change in body weight

A series of studies were conducted to investigate the treatment-induced body weight (BW) loss in both PDAC tumor-bearing mice and CD-1 immunocompetent mice. Body weight was measured daily or twice a week. As shown in Figure 2 and Table 2, maximum BW loss (percentage of mean maximum BW loss compared with pretreatment) in the T monotherapy group was 0, G + nP induced maximum BW loss from 4 to 16%, and the G + nP + T triplet did not induce more body weight loss compared to the G + nP doublet. With BW loss as a read-out, additive toxicity in triplet treatment compared with the doublet treatment was not evident.

No additional toxicity was observed on adding TH-302 to gemcitabine and nab-paclitaxel using hematological and liver function parameters as read-outs

The same treatments were employed in PANC-1 tumor-bearing nude mice as well as immunocompetent CD-1 mice. Twenty four hours after the last treatment, the animals were sacrificed with CO₂, blood was collected via heart puncture, and hematological analysis performed using a Hemavet 950 blood analyzer. As shown in Figure 3A and B, G + nP combination therapy or T monotherapy reduced neutrophils, lymphocytes, and monocytes, compared with V, but there was no additional decrease in neutrophil, lymphocyte, or monocyte counts when T was added to G + nP (compared to G + nP). The G + nP + T combination therapy did not add hemotoxicity compared with the G + nP combination therapy. Results obtained were consistent between the 2 models. A separate study conducted in CD-1

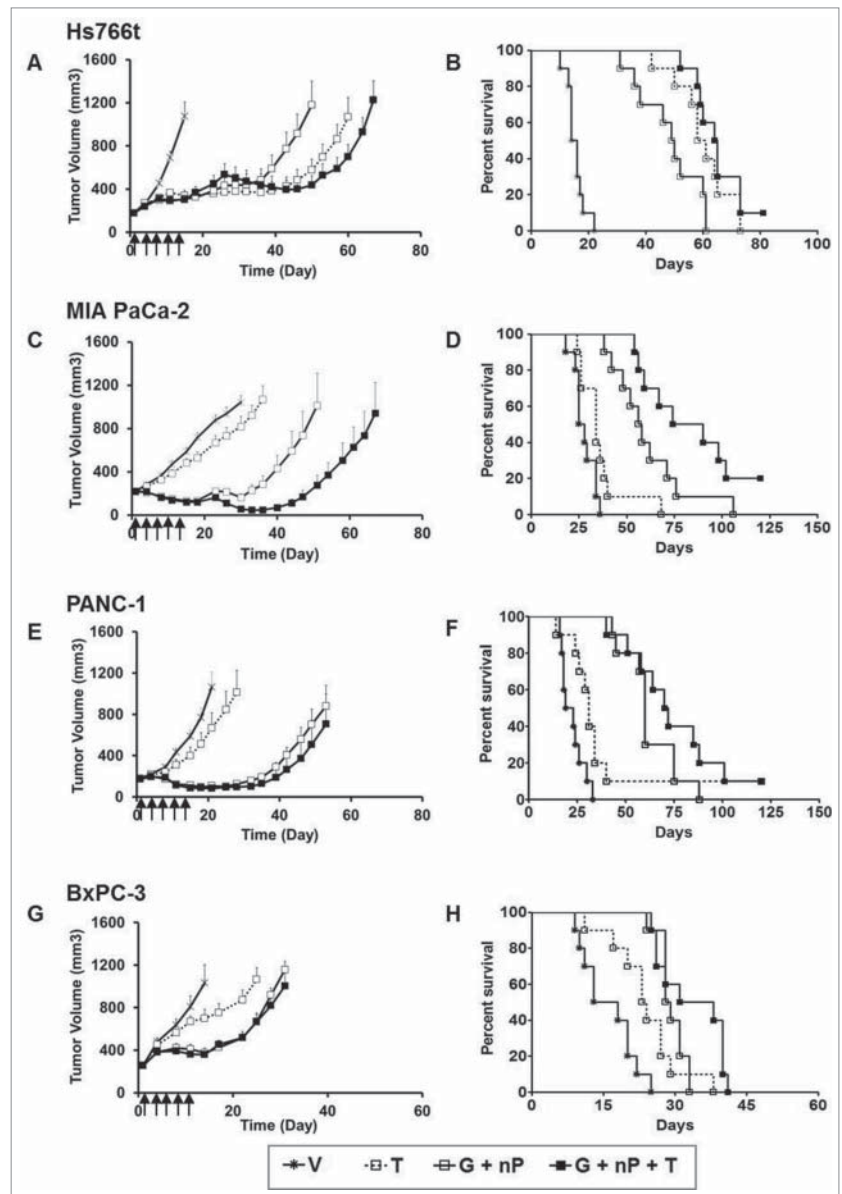


Figure 1. Antitumor efficacy of TH-302 (T) in combination with gemcitabine (G) and nab-paclitaxel (nP) in 4 PDAC xenograft models: Hs766t (A and B), MIA PaCa-2 (C and D), PANC-1 (E and F) and BxPC-3 (G and H), n = 10 for each group. T was given at 50 mg/kg, ip, G was given at 60 mg/kg ip and nP was given at 30 mg/kg, iv; all drugs were dosed at a Q3Dx5 regimen. A, C, E, and G, tumor growth was monitored and quantified twice a week. Data represent Mean ± SEM. B, D, F and H, Kaplan-Meier analysis plot using tumor size of 1000 mm³ as end-point. V, vehicle; Arrow, dosing time.

mice showed that by 30 days after the last treatment, all white blood cell parameters returned to normal levels (Fig. 3C).

To examine the effects of the different treatment regimens on liver and kidney function, blood samples from immunocompetent CD-1 mice were collected 24 hrs after the last treatment and plasma fractions were prepared. Plasma AST levels were elevated after G + nP combination therapy, and G + nP + T combination therapy did not further increase these liver function

Table 1. Summary of antitumor activity of TH-302 monotherapy, gemcitabine and nab-paclitaxel doublet and gemcitabine, nab-paclitaxel and TH-302 triplet in the Hs766t, MIA PaCa-2, PANC-1 and BxPC-3 PDAC xenograft models

Model	Group	TGI	TGD ₁₀₀₀ (vs. Vehicle)	CR Rate	TV 1000 mm ³ as Endpoint	
					MT (day)	ILS
Hs766t	Vehicle			0	15	
	TH-302	82%	47	0	60 ^{*a}	297%
	G + nP Doublet	85%	35	0	50*	230%
	G + nP + T Triplet	86%*	53	10%	65 ^{*a,b}	330%
MIA PaCa-2	Vehicle			0	27	
	TH-302	27%	6	0	34	26%
	G + nP Doublet	107%*	23	30%	57*	111%
	G + nP + T Triplet	120% ^{*a,b}	>39	90%	82 ^{*b}	204%
PANC-1	Vehicle			0	21	
	TH-302	45%	7	10%	31	48%
	G + nP Doublet	107%*	34	60%	60*	186%
	G + nP + T Triplet	110% ^{*a,b}	>34	100%	71 ^{*b}	238%
BxPC-3	Vehicle			0	16	
	TH-302	43%	11	0	24	52%
	G + nP Doublet	85%*	16	0	29*	84%
	G + nP + T Triplet	87% ^{*b}	18	0	35 ^{*b}	123%

TGI: Tumor Growth Inhibition; TGD₁₀₀₀: Tumor Growth Delay compared to Vehicle reaching the size of 1000 mm³; CR: complete response, the disappearance of measurable tumor mass or if measured tumor volume was less than 100 mm³ after initiating therapy; MT: Median Time to reach the size of 1000 mm³; ILS: Increased Life Span; *, p < 0.05 compared with Vehicle; ^a, p < 0.05 compared with G + nP Doublet; ^b, p < 0.05 compared with T monotherapy.

parameter levels. There was a significant elevation of ALT in the G + nP + T combination group compared with V. However, there was no statistical difference in ALT levels between the G + nP + T triplet combination compared to the G + nP doublet treated animals (Fig. 3D). There was no change in renal function parameters (BUN, creatinine) in any of the treated groups, compared with V (data not shown).

No additional toxicity was observed on adding TH-302 to gemcitabine and nab-paclitaxel assessed by von Frey neuropathy assay

Male CD-1 mice were used for mechanical hyperalgesia tests based on the von Frey neuropathy assay. As shown in Figure 4, at baseline, there were no differences in response to mechanical stimulus between mice in the 4 groups. However, 9 days after the initiation of the treatment, G + nP doublet combination treated mice exhibited a significant hind paw mechanical hyperalgesia compared to V controls ($P < 0.05$). This hyperalgesia persisted out to 37 days with peaks at day 16 and day 23 ($P < 0.001$), and gradually returned to the baseline at day 43. A similar change in mechanical hypersensitivity was observed in mice treated with the G + nP + T triplet combination compared to V over time. There was no difference between G + nP + T combination treated and G + nP combination treated animals. Of note, no mechanical hyperalgesia was detected in mice treated with T monotherapy in the various time points tested. The results suggest that the triplet of G + nP + T did not add neuropathy compared with the G + nP doublet combination.

TH-302 in combination with gemcitabine and nab-paclitaxel targets both cancer cells and stromal cells

We used a panel of histological and immunohistological markers to characterize Hs766t, MIA PaCa-2, PANC-1 and

BxPC3 xenograft tumors. The four tumor types showed different hypoxia levels, vasculature, EMT status, and stroma components (Fig. S2). We chose the medium hypoxic level tumor PANC-1 to study the pharmacodynamic changes induced by the different treatments. PANC-1 tumor-bearing animals were treated with V, T at 50 mg/kg alone, G + nP (60 mg/kg, ip and 30 mg/kg iv, respectively), and G + nP + T when tumor size was approximately 500 mm³ with a Q3Dx5 dosing regimen. One day after the last treatment, tumors were harvested, paraffin-embedded, and sectioned for the staining of histology and immunohistochemistry biomarkers. Representative assessments of necrosis, apoptosis, DNA damage, and proliferation of the tumor cells with or without treatment are shown in Figure 5A, and morphometric analysis results are shown in Figure 5B-F. Tumor necrotic fraction was significantly increased to 64% after the G + nP + T triplet combination, compared with 9% in V, 35% in T alone, and 33% in the G + nP doublet group ($P < 0.01$). Apoptotic cells, detected by TUNEL assay, were observed in both cancer cell, and in the stromal compartment in the non-necrotic regions. G + nP + T triplet therapy significantly increased the number of apoptotic cells (8.0 ± 0.3 per field, compared to 0.8 ± 0.1 , 3.0 ± 0.2 , 6.3 ± 0.5 , in V, T alone and G + nP, respectively, $P < 0.05$). A similar trend was observed when using Caspase-3 as another apoptosis biomarker. γ H2AX foci formation analysis was employed to assess treatment induced DNA damage. Similar to the results observed for apoptosis, γ H2AX-positive cells were increased in all 3 drug-treated groups compared with V: 31 ± 1.3 positive cells/field in the G + nP + T triplet group compared with 20 ± 2.1 in T alone, 19 ± 2.2 in G + nP, or 4 ± 0.4 in V ($P < 0.05$). Cells with DNA damage were evenly distributed in both the hypoxic and oxic compartments in non-necrotic regions after the G + nP + T triplet treatment. Ki67 is a marker of cell proliferation and labels all active phases of the cell cycle including S, G₂, and mitosis.

Immunostaining demonstrated that Ki67-positive cells were significantly reduced after drug treatment but reduced by a greater magnitude in the G + nP + T triplet combination group.

Representative images of the tumor micro-environment including tumor stroma and hypoxia are presented in **Figure 6A**. Tumor stroma is composed of extracellular matrix protein and cellular elements. Collagen I and III, major components of extracellular matrix, were evaluated by Picosirius red staining. Activated fibroblasts in the stroma were analyzed by α -SMA staining. By morphometric analysis (**Fig. 6B-C**), G + nP significantly reduced extracellular collagen and α -SMA expression, and no further reduction was observed in the G + nP + T group. T-alone had no effect on α -SMA or collagen expression compared to V. Of note, after treatment of G + nP or G + nP + T, the thinner, disrupted, and disorganized collagen appeared by Picosirius red staining, relative to V. Hypoxic regions in the tumors were detected by pimonidazole immunostaining. Morphometric analysis showed T alone did not reduce the hypoxic fraction (HF, $10.6 \pm 1.1\%$ vs. $12.4 \pm 2\%$ in V); however, the triplet with T significantly reduced the hypoxic level, with HF of $2.5 \pm 0.5\%$, compared with $7.1 \pm 1.7\%$ in G + nP group ($P < 0.05$) (**Fig. 6D**). There was no co-localization between exogenous pimonidazole- and endogenous CAIX-positive cells (**Suppl. Fig. 3**), and CA IX was observed in necrotic cells as well. Pimonidazole and Caspase-3 immunostaining was performed on consecutive sections. As shown in **Figure 6E**, there were very low levels of Caspase-3 positive cells observed in V treated tumors. TH-302 induced Caspase-3 positivity was significantly increased and mainly located in the hypoxia zone, while further increased apoptotic cells by G + nP treatment were mainly in the normoxic (oxic) compartment. The triplet of G + nP + T resulted in apoptotic cells throughout the tumor (**Fig. 6E**).

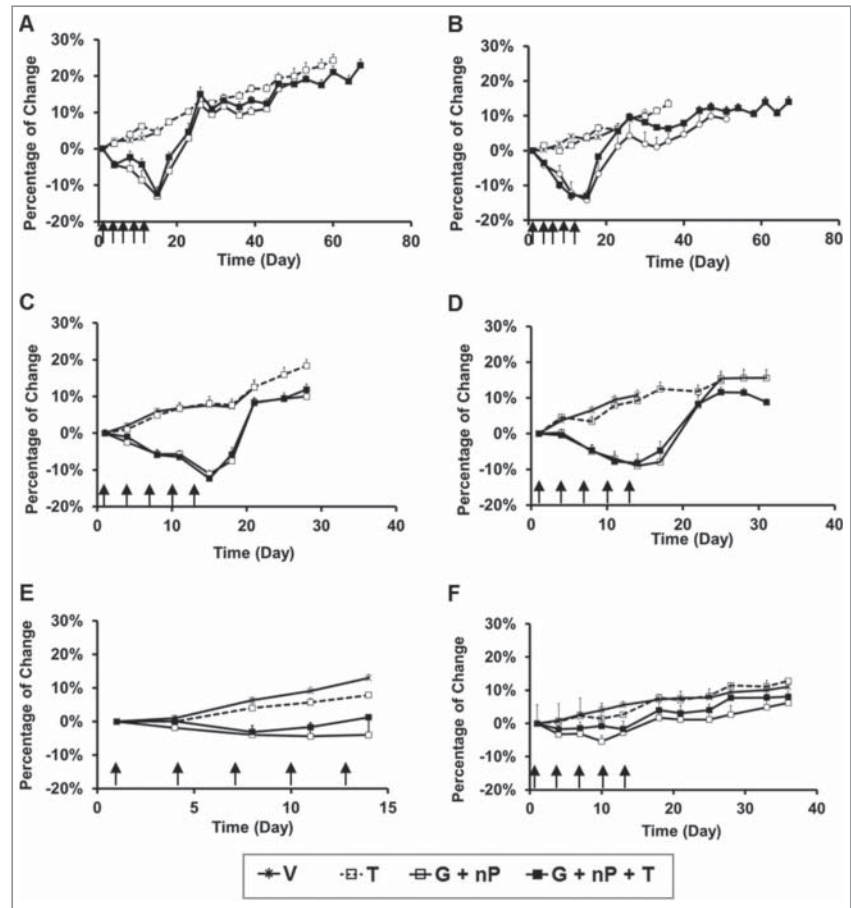


Figure 2. Body weight change of animals treated with TH-302 (T) in combination with gemcitabine (G) and nab-paclitaxel (nP) in tumor-bearing immunocompromised mice and immunocompetent mice. T was given at 50 mg/kg, ip, G was given at 60 mg/kg ip and nP was given at 30 mg/kg, iv; all drugs were dosed at a Q3Dx5 regimen. (**A-D**), in Hs766t, MIA PaCa-2, PANC-1 and BxPC-3 tumor-bearing nu/nu mice, respectively, $n = 10$ per group; (**E**), in CD-1 female mice, $n = 6$ per group; and (**F**), in CD-1 male mice, $n = 10$ per group. Data represent Mean \pm SEM. Arrow, dosing time.

Discussion

These studies evaluated the efficacy and safety profile of the combination of nab-paclitaxel, gemcitabine, and TH-302. We used a series of preclinical PDAC xenograft model-based studies to demonstrate the superior efficacy and safety profile of the

Table 2. Summary of TH-302 monotherapy, gemcitabine and nab-paclitaxel doublet, and gemcitabine, nab-paclitaxel and TH-302 triplet induced maximal body weight loss in the PDAC tumor bearing nu/nu and non-tumor bearing CD-1 immunocompetent mice

Cell Line	Hs766t	MIA PaCa-2	PANC-1	BxPC3	Non-tumor	Non-tumor
Mouse Strain	nu/nu	nu/nu	nu/nu	nu/nu	CD-1	CD-1
Sex	Female	Female	Female	Female	Female	Male
# of Animal/group	$n = 10$	$n = 10$	$n = 10$	$n = 10$	$n = 6$	$n = 10$
Vehicle	0	0	0	0	0	0
T	0	0	0	0	0	0
G + nP Doublet	13% (Day 15)	14.2% (Day 15)	11.1% (Day 15)	9% (Day 14)	4.2% (Day 11)	5.4% (Day 10)
G + nP + T Triplet	12.3% (Day 15)	13% (Day 15)	12.3% (Day 15)	8.2% (Day 11)	3% (Day 8)	1.7% (Day 14)

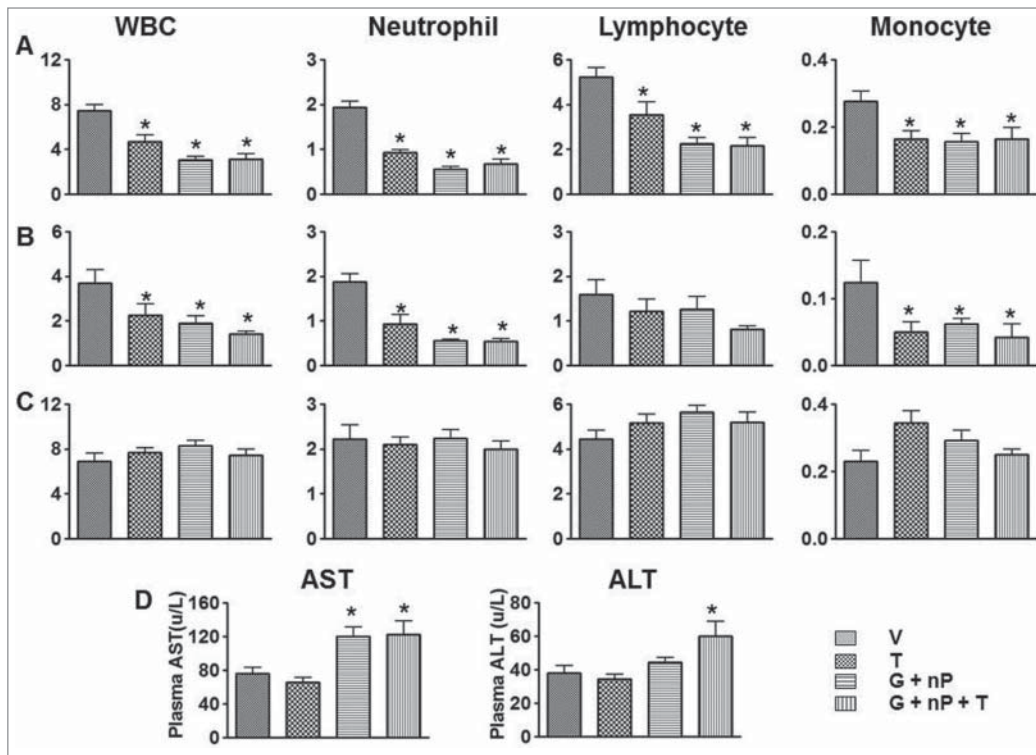


Figure 3. Effect of TH-302 (T) in combination with gemcitabine (G) and nab-paclitaxel (nP) on hematologic change and blood chemistry changes PANC-1 tumor bearing nude mice and CD1 mice. The means and standard errors from the 6 mice per group are presented. (A) blood samples were collected 24 hrs after the last treatment from non-tumor bearing CD-1 mice. (B) blood samples were collected 24 hrs after the last treatment from PANC-1 bearing nude mice. (C), blood samples were collected 30 days after the last treatment from non-tumor bearing CD-1 mice. (A-C), y axis label is cell number ($\times 10^3/\mu\text{l}$). (D), plasma samples were collected 24 hrs after the last treatment from non-tumor bearing CD-1 mice. T was given at 50 mg/kg, ip, G was given at 60 mg/kg ip and nP was given at 30 mg/kg, iv; all drugs were dosed at a Q3Dx5 regimen. *, $P < 0.05$ as compared to Vehicle (V).

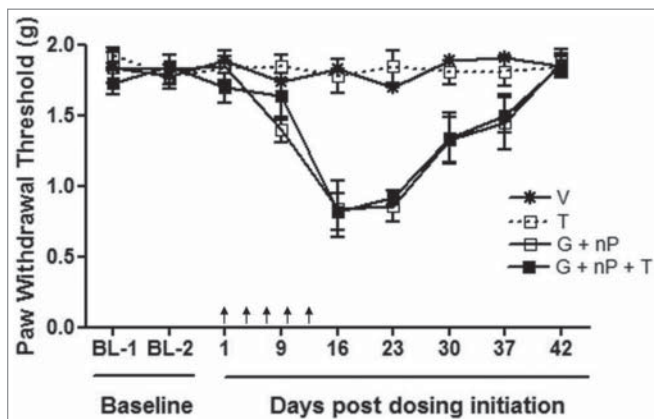


Figure 4. Effect of TH-302 (T) in combination with gemcitabine (G) and nab-paclitaxel (nP) on mechanical hyperalgesia, analyzed by von Frey Assay. T was given at 50 mg/kg, ip, G was given at 60 mg/kg ip and nP was given at 30 mg/kg, iv; all drugs were dosed at a Q3Dx5 regimen. Data represent Mean \pm SEM of 10 male CD-1 mice each group. Arrow, dosing time.

triplet combination, compared with the gemcitabine and nab-paclitaxel doublet combination.

Mimicking the clinical trial design, a tolerable dose of TH-302 was administered with the MTD of the gemcitabine and nab-paclitaxel doublet. Thus 50 mg/kg of TH-302 every-3-days were administered, which is half the monotherapy MTD dose. The G + nP doublet showed good antitumor activity in all 4 models, with TGIs ranging from 85% to 107%. When TH-302 was added to the doublet, an enhanced efficacy profile was observed in a variety of different parameters, including the inhibition of tumor growth, delayed tumor regrowth after the treatment period ended, and increased complete response rate. By immunohistochemistry and histology staining, we found that apoptosis and DNA damage were significantly increased and cell proliferation reduced after the triplet therapy compared with doublet therapy.

As a consequence, the necrotic region in triplet treated tumors was significantly enlarged. The studies provide a translational basis for combining gemcitabine, nab-paclitaxel, and TH-302 therapies in the clinical setting.

Tumor growth is dependent on complex interactions between multiple components, including tumor cells as well as the endothelial cells and fibroblasts in the stroma that promote tumor growth. Combining conventional cytotoxic drugs with novel targeted agents has recently gained much attention in the effort to identify novel, more effective, and less toxic PDAC treatments. Chemotherapy resistance to gemcitabine is one of the reasons underlying poor outcomes in patients. PDAC tumor stroma serves as a mechanical barrier and promotes tumor formation, progression, invasion, and metastasis development.³²⁻³⁴ Treatment with nab-paclitaxel alone or nab-paclitaxel in combination with gemcitabine has been shown to decrease cancer-associated fibroblast (CAF) content, inducing a marked alteration in cancer stroma that result in tumor softening both preclinically²⁹ and clinically²⁸. In our studies, we also found that the G + nP doublet significantly reduced the number of α -SMA positive fibroblasts as well as reduced extracellular collagen. The triplet did not further reduce the fibroblast numbers, suggesting a minor effect,

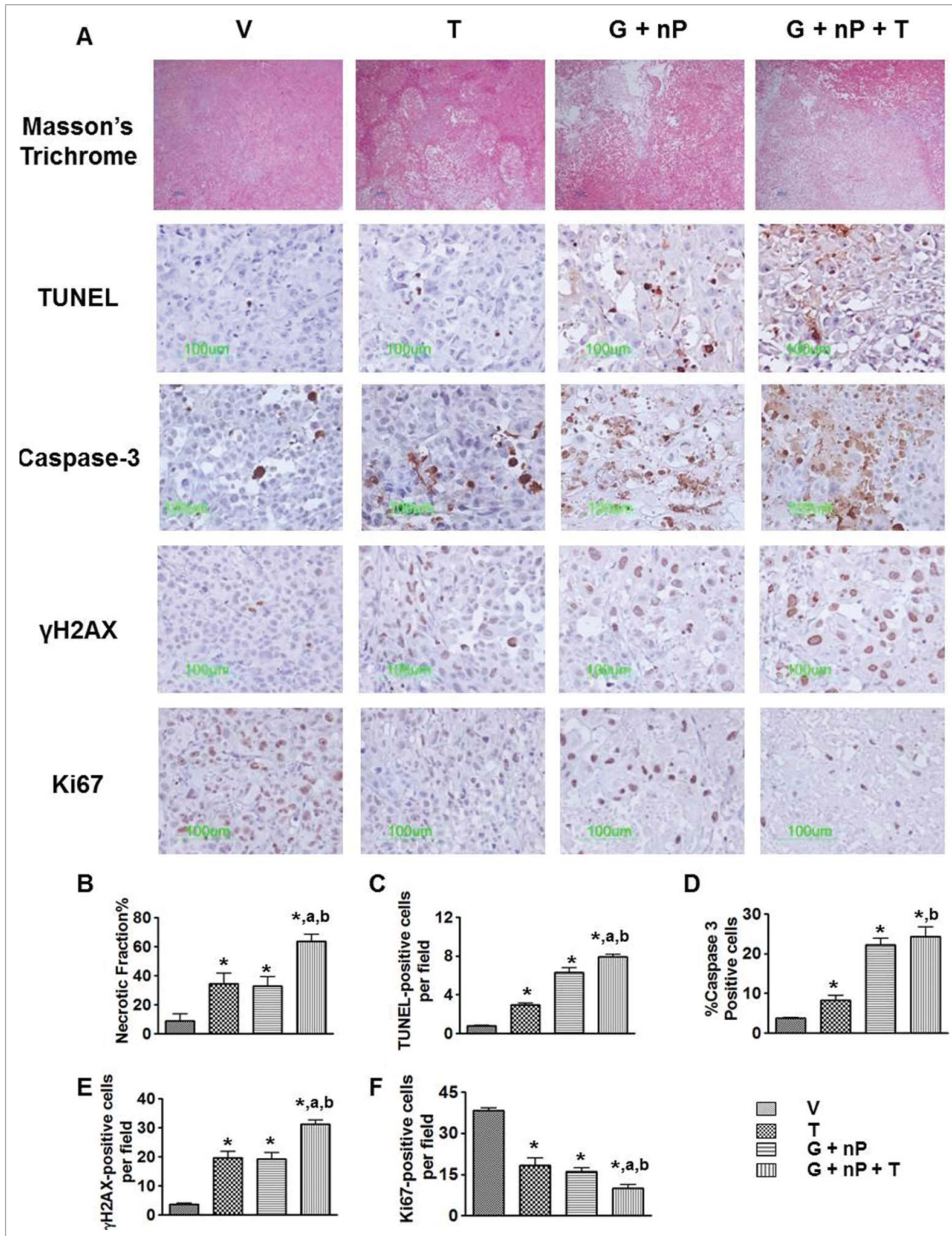


Figure 5. Effect of TH-302 (T) in combination with gemcitabine (G) and nab-paclitaxel (nP) on tumor cells. PANC-1 tumor bearing animals received T, 50 mg/kg, ip; G, 60 mg/kg ip; and nP 30 mg/kg, iv, at a Q3Dx5 regimen. Tumors were collected 24 hrs after the last treatment. (A), representative images of Masson's Trichrome histology staining, TUNEL staining, Caspase-3, γ H2AX, and Ki67 immunostaining in vehicle (V), T alone, G + nP doublet and G + nP + T triplet groups. Morphometric analysis of (B), necrotic fraction in the whole tumor by Masson's Trichrome; (C), number of TUNEL-positive apoptotic cells; (D), percentage of Caspase-3 positive apoptotic cells; (E), number of γ H2AX positive DNA damage cells; and (F) number of Ki67 positive proliferative cells. *, $P < 0.05$ as compared to Vehicle (V). ^a, $P < 0.05$ as compared to G + nP; ^b, $P < 0.05$ as compared to T alone.

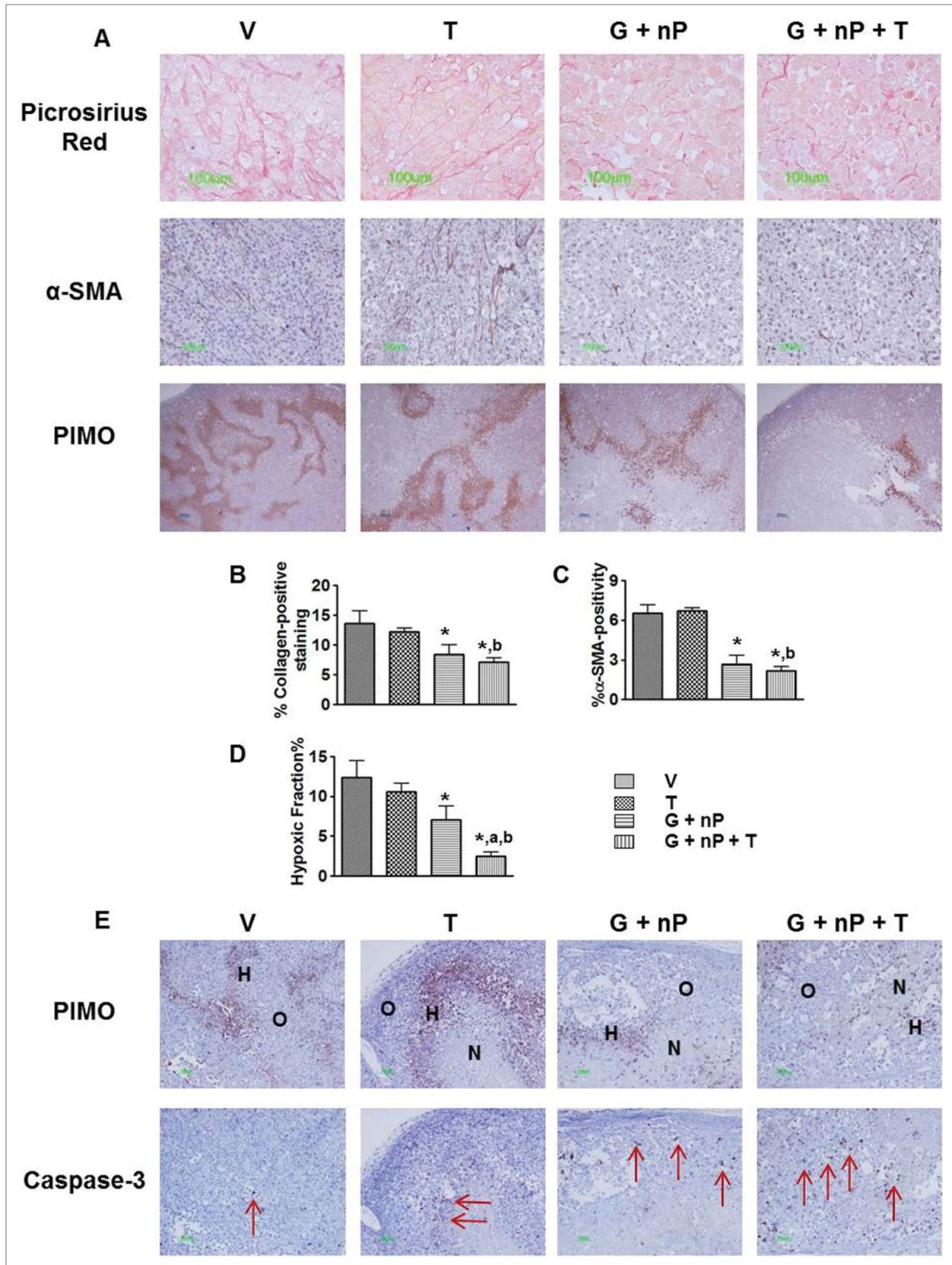


Figure 6. For figure legend, see page 446.

if any, of TH-302 on collagen or fibroblasts. The gemcitabine and nab-paclitaxel doublet significantly reduced the hypoxic fraction of tumor. This effect might be related to the activity of these conventional chemotherapeutics on normoxic cells that results in a reduction of oxygen consumption and a concomitant re-oxygenation of hypoxic compartment.^{35,36} As a single agent, 50 mg/kg of TH-302 did not decrease the hypoxic fraction in PANC-1 xenograft tumors, whereas in previous studies we demonstrated that a higher dose of 150 mg/kg TH-302 reduced the hypoxic fraction in several xenograft models including Hs766t xenografts.²⁰ One of the reasons for the observed difference in effect could be the lower dose of TH-302 used in the current study. Interestingly, we did see that adding TH-302 reduced the hypoxic fraction relative to that of G + nP doublet. In published preclinical studies, exposure to nab-paclitaxel collapsed the PDAC stroma and as a result, intratumoral concentration of gemcitabine was increased.^{29,37} It is possible that nab-paclitaxel increases the intratumoral concentration of TH-302 in a similar manner. As a consequence, exposure to TH-302 could then be high enough to target hypoxic regions selectively and reduce the hypoxic fraction when the lower TH-302 dose is administered in the triplet. Numerous studies have demonstrated an association between the magnitude of intratumoral hypoxia and the outcome of cancer treatment.³⁻⁸ This association has also been shown for PDAC, where a more hypoxic phenotype is associated with a worse prognosis.^{38,39} We hypothesize that the clinical outcome for patients treated with the triplet treatment may be more favorable than doublet nab-paclitaxel and gemcitabine, given the multiple therapeutic modalities employed including hypoxia-selective targeting.

In the Phase 3 trial of gemcitabine in combination with nab-paclitaxel in metastatic PDAC patients, the most common adverse events of grade 3 or higher were neutropenia (38% in the nab-paclitaxel-gemcitabine group vs. 27% in the gemcitabine group), fatigue (17% vs. 7%), and neuropathy (17% vs. 1%).²⁷ Here we used PANC-1 tumor bearing nude mice and CD-1 mice to demonstrate the safety profile of the triplet. The results showed that adding TH-302 to the G + nP doublet did not induce further body weight loss or further reductions in neutrophil, lymphocyte, or platelet counts compared with those observed with the G + nP doublet. Not only taxanes, but a number of chemotherapeutic agents also induce neuropathy, including cisplatin, oxaliplatin, ifosfamide, vinca alkaloids, etoposide.⁴⁰ Given the fact that the cytotoxic effector of TH-302 is structurally very similar to that of ifosfamide,¹⁸ we tested whether TH-302 might cause neuropathy as a monotherapy or add more neurotoxicity when combined with gemcitabine and nab-paclitaxel. We used

immunocompetent CD-1 mice to conduct mechanical hyperalgesia tests by the von Frey Assay as a preclinical model of peripheral neuropathy. To our knowledge, this is the first report of nab-paclitaxel and gemcitabine combination-induced neuropathy in mice. Consistent with the other safety profiling observations described, the addition of TH-302 did not add to the neuropathy observed in the G + nP doublet. Overall, toxicity attributable to TH-302 was minimal, and there was no evidence of additive toxicity when TH-302 was added to the gemcitabine and nab-paclitaxel doublet.

In summary, 4 PDAC models, Hs766t, PANC-1, MIA PaCa-2 and BxPC-3, were used to study the triplet of G + nP + T in comparison to G + nP doublet or TH-302 monotherapy. A statistically significant difference in antitumor activity was observed between the triplet of G + nP + T and the G + nP doublet in the Hs766t, MIA PaCa-2, and PANC-1 models based on TGI and Kaplan-Meier survival time. The triplet of G + nP + T did not increase the safety markers of body weight loss, hematologic toxicity, hepatotoxicity, or neuropathy compared with the G + nP doublet. This favorable preclinical antitumor activity and safety profile of the triplet G + nP + T against PDAC supports exploration of this regimen in human clinical trials. A Phase I dose escalation study assessing the tolerability and anti-tumor activity of TH-302 in combination gemcitabine and nab-paclitaxel in patients with previously untreated, locally advanced unresectable or metastatic pancreatic adenocarcinoma has been initiated (NCT02047500).

Materials and Methods

Compounds

TH-302 was synthesized by Syngene (Bangalore). Gemcitabine for Injection (38 mg/ml) (Hospira) and nab-paclitaxel (Abraxane[®]) for Injectable Suspension (Celgene) were purchased. All three compounds were formulated or diluted in saline (0.9% NaCl). TH-302 solution was filtered through 0.2 μ m filter prior to dosing.

Cell lines

Hs766t, MIA PaCa-2, PANC-1, and BxPC-3 were obtained from the American Type Culture Collection (ATCC). Cells were cultured in the ATCC-suggested media with 10% fetal bovine serum added and maintained in a 5% CO₂, humidified environment at 37°C.

Figure 6 (See previous page). Effect of TH-302 (T) in combination with gemcitabine (G) and nab-paclitaxel (nP) on tumor microenvironment. PANC-1 tumor bearing animals received T, 50 mg/kg, ip; G, 60 mg/kg ip; and nP 30 mg/kg, iv, at a Q3Dx5 regimen. Tumors were collected 24 hrs after the last treatment. **(A)**, representative images of Picrosirius red histology staining, α -smooth muscle actin (α -SMA) and pimonidazole immunostaining in vehicle (V), T alone, G + nP doublet and G + nP + T triplet groups. Morphometric analysis of **(B)** percentage of extracellular collagen by Picrosirius red staining; **(C)** percentage of α -SMA positivity inside the tumor; and **(D)** hypoxic fraction in the whole tumor by pimonidazole immunostaining. *, $p < 0.05$ as compared to Vehicle (V). ^a, $P < 0.05$ as compared to G + nP; ^b, $P < 0.05$ as compared to T alone. **(E)**, representative images of pimonidazole and Caspase-3 immunostaining on consecutive sections. H, hypoxic compartment; O, oxalic compartment; N, necrotic region; arrow, indicating the positive cells.

Experimental animals

Homozygous female nude mice (Nu-Foxn 1^{nu} NU/NU, Charles River Laboratories) were used for the xenograft models. Mice were given food and water *ad libitum* and housed in micro-isolator cages. Four- to 6-week-old animals were tagged with microchips (Locus Technology) for identification.

CD-1 mice (Charles River Laboratories) were used for MTD determination and safety profiling investigation (females 5 weeks old or males aged 9 weeks). All animal studies were approved by the Institutional Animal Care and Use Committee of Threshold Pharmaceuticals.

Drug treatments

In the Phase 2 (NCT01144455) and Phase 3 clinical trials (NCT01746979) of the TH-302 (T) and gemcitabine (G) doublet, T was administered first and then followed by G 2 hrs later on Days 1, 8 and 15 of a 28-day cycle. Similarly, nab-paclitaxel (nP) is administered followed by G with the same regimen in the Phase 3 trial of the nP and G doublet (NCT00844649). An administration of T, nP, and G with a Q3Dx5 regimen was utilized in these preclinical studies. We have shown that T given 2–4 hrs before administration of conventional chemotherapeutics is an optimal schedule.²¹ nP prior to G is employed in both clinical²⁷ and preclinical settings,³⁷ and it has been shown that nP is able to increase intratumoral concentration of G.³⁷ In this study, the animals were first dosed with TH-302 ip, followed by nP iv 2 hrs later, and then after 1 more hr, G was given ip. MTD was determined by dose escalations in a small number of CD-1 immunocompetent mice or non-tumor bearing nu/nu mice. The MTD was defined as the highest dose resulting in no animal deaths, less than 20% weight loss for any one animal in an experimental group, no significant changes in general clinical signs, and no abnormal gross anatomical findings after necropsy. General clinical signs included: respiratory rate, behavior, and response to normal stimuli.⁴¹ MTDs of 50 mg/kg of T, 30 mg/kg of nP, and 60 mg/kg of G were determined.

Xenograft models and *in vivo* antitumor activity

5×10^6 human cancer cells mixed 1:1 with Matrigel (BD Bioscience) in a total volume of 0.2 ml were implanted to the subcutaneous area of the flank of the nude mouse.

Tumor growth and body weight were measured twice a week after cell implantation. Tumor volume was calculated as $(\text{length} \times \text{width}^2)/2$. When the mean value of tumor volume was approximately 150 mm³, mice were randomized into 10 mice per group and the treatment started (Day 1). Antitumor activity was assessed by Tumor Growth Inhibition (TGI) and Tumor Growth Delay (TGD). TGI was defined as $(1 - \Delta T / \Delta C) \times 100$, where $\Delta T / \Delta C$ is the ratio of the change in mean tumor volume of the treated group (ΔT) to that of the control group (ΔC). Animals were euthanized when tumor size was over 2000 mm³ or tumor size was over 1000 mm³ if mean tumor volume exceeded. TGI was determined on the last measurement taken with all animals in the vehicle group still alive. TGD₁₀₀₀ was determined as the increased time (in days) for the treated groups' tumor size on average to reach 1000 mm³ as compared to the vehicle group,

using the tumor growth curves. A complete response (CR) was defined as the disappearance of measurable tumor mass or if measured tumor volume was less than 100 mm³ after initiating therapy.⁴² Data are expressed as the mean \pm SEM. One-way analysis of variance with Dunnett's test (GraphPad PRISM 4) was used for analysis. A *p* level < 0.05 was considered statistically significant. Conditional survival was defined as the time that an animal reached the endpoint of a tumor size of 1000 mm³. Kaplan-Meier plots were constructed based on the percentage animals surviving in each group as a function of time. Median time (MT) is the time at which half the animals in the group had a tumor size less than 1000 mm³. The antitumor activity was evaluated as follows: T/C % = MT of treated group/MT of control group \times 100. Results were also expressed as the percentage of increased life span (ILS, T/C of treated group – 100). Statistical significance between the groups was evaluated by the log-rank test.

Hematological parameters and blood chemistry assays

PANC-1 tumor-bearing nude mice or CD-1 female mice (5 mice per group) were used. Twenty four hours after the last treatment, animals were euthanized, and blood from each animal was immediately withdrawn by cardiac puncture into EDTA-containing tubes. Blood samples were immediately analyzed for hematological parameters with a Hemavet 950 (Drew Scientific) and also centrifuged at 5000 r.p.m. for 5 minutes to collect plasma fraction for liver and kidney function tests.

Assay of mechanical hyperalgesia

Nine weeks old male CD-1 mice were randomly divided into 4 groups (10 per group) and allowed to habituate to the animal facility for one week prior to the study. Mechanical hyperalgesia tests were performed at 1 and 2 days prior to the initial drug treatment and 1, 9, 16, 23, 30, 37, and 44 days after treatment initiation by an observer blinded to animal identities.

Mechanical hyperalgesia was assayed using nylon von Frey filaments according to the "up-down" algorithm as described.⁴³ In this study, mice were placed individually in a plastic cage with a wire mesh bottom (IITC Life Science). After 20–30 minutes of acclimation, calibrated von Frey fibers (Stoelting) of sequentially increasing stiffness (0.16, 0.2, 0.4, 1, and 2 g) were applied against the right hind paw plantar skin at approximately midsole, taking care to avoid the tori pads, and pressed upward to cause a slight bend in the fiber and left in place for 5 sec. Withdrawal of or licking the hind paw after fiber application is scored as a response. When no response is obtained, the next stiffest fiber in the series is applied to the same paw; if a response is obtained, a less stiff fiber is applied. Testing proceeds in this manner until 4 fibers have been applied after "negative + positive or positive + negative" response. Estimation of the mechanical threshold to withdraw (grams) by data fitting algorithm permits the use of parametric statistics for analysis.⁴⁴

Behavioral data collected over time after the injection of drug were analyzed statistically using a 2-way analysis of variance (ANOVA) followed by Bonferroni post hoc tests for multiple-comparison testing to compare various treatment groups with

vehicle for each test time point. All data are presented as mean \pm SEM, and differences are considered significant at a *p* value less than 0.05 (Prism 6, GraphPad Software).

Histological and immunohistochemical analyses

PANC-1 tumor bearing animals were randomly divided into groups (5 per group) when tumor size was approximately 500 mm³. Tumors were harvested one day after the last treatment. The hypoxia biomarker pimonidazole hydrochloride (HP-1000, Hypoxyprobe) was intraperitoneally (ip) injected one hour before animal sacrifice at 60 mg/kg. Tumors were harvested, fixed in 10% neutral buffered formalin, and embedded in paraffin. Masson's Trichrome and Picrosirius red stainings were conducted for tumor morphology and extracellular collagen, respectively. For immunohistochemistry, paraffin-embedded slides were deparaffinized and rehydrated. Antigen retrieval was performed using Heat Induced Epitope Retrieval Buffer (DV2004MX, Biocare Medical) in Decloaker Chamber (Biocare Medical). Slides were incubated with the primary antibodies for 1 hr at RT followed by secondary HRP-conjugated anti-rabbit IgG (ab137913, Abcam). The primary antibodies included rabbit polyclonal anti-pimonidazole (HP3-1000, Natural Pharmacia International, 1:400), rabbit polyclonal anti-cleaved Caspase-3 (9661, Cell Signaling, 1:300), rabbit monoclonal anti- γ H2AX (ab81299, Abcam, 1:3000), rabbit monoclonal anti-Ki67 (ab16667, Abcam, 1:2000), and rabbit monoclonal anti- α -smooth muscle actin (α -SMA, ab781, Abcam, 1:2000).

Terminal uridine deoxynucleotidyl transferase-mediated dUTP nick end labeling (TUNEL) staining with the ApopTag Peroxidase In Situ Apoptosis Detection Kit (S7100, Millipore) was used to detect apoptotic cells.

Image analysis

With a 20x objective, digital images of Masson's Trichrome stained or pimonidazole stained sections were captured and assembled to compose a whole tumor image (Nikon TS-100). The necrotic fraction (NF) in the individual tumor was calculated as the percentage of the necrotic area in the whole tumor section. Pimonidazole positive regions were extracted using Image-Pro Plus v6.0 (MediaCybernetics). The hypoxic fraction (HF) was determined as the percentage of pimonidazole-

positive hypoxic area in the whole tumor. All images were captured under consistent illumination and exposure for their respective stains. No image post-processing was done. Custom-made scripts were developed in Image Pro-Plus to analyze the target signals using color and morphologic segmentation tools. For semi-quantification of α -SMA- positive area and extracellular collagen, point counting was performed. A total of 10 to 15 fields at 400x magnification, per section, were counted in each animal on a 1-cm² eyepiece graticule with 10 equidistant grid lines. The percentage of fractional area (percentage of positive area per total area counted of the section) was calculated using the following formula: percentage of positive fractional area = number of grid intersections with positive staining / total number of grid intersections multiplied \times 100%. γ H2AX, apoptotic or Ki67 positive cells were counted at 400x magnification. Ten fields per section were used, and data were presented as the number of positive cells per field. Caspase-3 positive cells in each section were counted at 400x magnification from 10 fields. Percentage of positive cells was calculated as number of positive cells/number of total cells \times 100. Statistical analysis was used in all instances, with a *p* value $<$ 0.05 considered significant. One-way analysis of variance with Dunnett's test (GraphPad PRISM 4) was used to compare the significance of the multiple groups. The Student's *t*-test was used to find the significance between 2 groups.

Disclosure of Potential Conflicts of Interest

This research was funded by Threshold Pharmaceuticals, Inc. and Merck KGaA. J Sun, Q Liu, D Ahluwalia, F Meng, Y Wang, D Bhupathi and C Hart are employees of Threshold Pharmaceuticals, Inc.. and hold either stock or stock options in the company. W Li is a paid consultant to Threshold, and A Ruprell is a former summer intern at Threshold.

Supplemental Material

Supplemental data for this article can be accessed on the publisher's website.

References

- Harris AL. Hypoxia—a key regulatory factor in tumour growth. *Nat Rev Cancer* 2002; 2:38-47; PMID:11902584; <http://dx.doi.org/10.1038/nrc704>
- Bertout JA, Patel SA, Simon MC. The impact of O₂ availability on human cancer. *Nat Rev Cancer* 2008; 8:967-75; PMID:18987634; <http://dx.doi.org/10.1038/nrc2540>
- Benito J, Zeng Z, Konopleva M, Wilson WR. Targeting hypoxia in the leukemia microenvironment. *Int J Hematol Oncol* 2013; 2:279-88; PMID:24490034; <http://dx.doi.org/10.2217/ijh.13.32>
- McKeown SR. Defining normoxia, physoxia and hypoxia in tumours-implications for treatment response. *Br J Radiol* 2014; 87:20130676; PMID:24588669; <http://dx.doi.org/10.1259/bjr.20130676>
- Vaupel P, Mayer A. Hypoxia in cancer: significance and impact on clinical outcome. *Cancer Metastasis Rev* 2007; 26:225-39; PMID:17440684; <http://dx.doi.org/10.1007/s10555-007-9055-1>
- Brizel DM, Scully SP, Harrelson JM, Layfield LJ, Bean JM, Prosnitz LR, Dewhirst MW. Tumor oxygenation predicts for the likelihood of distant metastases in human soft tissue sarcoma. *Cancer Res* 1996; 56:941-43; PMID:8640781
- Nordmark M, Overgaard M, Overgaard J. Pretreatment oxygenation predicts radiation response in advanced squamous cell carcinoma of the head and neck. *Radiother Oncol* 1996; 41:31-9; PMID:8961365; [http://dx.doi.org/10.1016/S0167-8140\(96\)91811-3](http://dx.doi.org/10.1016/S0167-8140(96)91811-3)
- Movsas B, Chapman JD, Hanlon AL, Horwitz EM, Greenberg RE, Stobbe C, Hanks GE, Pollack A. Hypoxic prostate/muscle pO₂ ratio predicts for biochemical failure in patients with prostate cancer: preliminary findings. *Urology* 2002; 60:634-9; PMID:12385924; [http://dx.doi.org/10.1016/S0090-4295\(02\)01858-7](http://dx.doi.org/10.1016/S0090-4295(02)01858-7)
- Subarsky P, Hill RP. The hypoxic tumour microenvironment and metastatic progression. *Clin Exp Metastasis* 2003; 20:237-50; PMID:12741682; <http://dx.doi.org/10.1023/A:1022939318102>
- Coquelle A, Toledo F, Stern S, Bieth A, Debatisse M. A new role for hypoxia in tumor progression: induction of fragile site triggering genomic rearrangements and formation of complex DMs and HSRs. *Mol Cell* 1998; 2:259-65; PMID:9734364; [http://dx.doi.org/10.1016/S1097-2765\(00\)80137-9](http://dx.doi.org/10.1016/S1097-2765(00)80137-9)
- Mimura I, Tanaka T, Wada Y, Kodama T, Nangaku M. Pathophysiological response to hypoxia - from the molecular mechanisms of malady to drug discovery: epigenetic regulation of the hypoxic response via hypoxia-inducible factor and histone modifying enzymes. *J Pharmacol Sci* 2011; 115:453-8; PMID:21422728; <http://dx.doi.org/10.1254/jphs.10R19FM>
- Graeber TG, Osmanian C, Jacks T, Housman DE, Koch SJ, Lowe SW, Giaccia AJ. Hypoxia-mediated

- selection of cells with diminished apoptotic potential in solid tumors. *Nature* 1996; 379:88-91; PMID:8538748; <http://dx.doi.org/10.1038/379088a0>
13. Cosse JP, Michiels C. Tumour hypoxia affects the responsiveness of cancer cells to chemotherapy and promotes cancer progression. *Anticancer Agents Med Chem* 2008; 8:790-7; PMID:18855580; <http://dx.doi.org/10.2174/187152008785914798>
 14. Phillips RJ, Mestas J, Gharace-Kermani M, Burdick MD, Sica A, Belperio JA, Keane MP, Strieter RM. Epidermal growth factor and hypoxia-induced expression of CXCR4 chemokine receptor 4 on non-small cell lung cancer cells is regulated by the phosphatidylinositol 3-kinase/PTEN/AKT/mammalian target of rapamycin signaling pathway and activation of hypoxia inducible factor-1alpha. *J Biol Chem* 2005; 280:473-81; PMID:15802268; <http://dx.doi.org/10.1074/jbc.M500963200>
 15. Vaupel P. The role of hypoxia-induced factors in tumor progression. *Oncologist* 2004; 9(suppl 5):10-7; PMID:15591418; <http://dx.doi.org/10.1634/theoncologist.9-90005-10>
 16. Gupta R, Chetty C, Bhoopathi P, Lakka S, Mohanam S, Rao JS. Downregulation of uPA/uPAR inhibits intermittent hypoxia induced epithelial-mesenchymal transition (EMT) in DAOY and D283 medulloblastoma cells. *Int J Oncol* 2011; 38:733-44; PMID:21181094
 17. Taddei ML, Giannoni E, Comito G, Chiarugi P. Microenvironment and tumor cell plasticity: an easy way out. *Cancer Lett* 2013; 341:80-96; PMID:23376253; <http://dx.doi.org/10.1016/j.canlet.2013.01.042>
 18. Duan JX, Jiao H, Kaizerman J, Stanton T, Evans JW, Lan L, Lorente G, Banica M, Jung D, Wang J, et al. Potent and highly selective hypoxia-activated acirhal phosphoramidate mustards as anticancer drugs. *J Med Chem* 2008; 51:2412-20; PMID:18257544; <http://dx.doi.org/10.1021/jm701028q>
 19. Meng F, Evans JW, Bhupathi D, Banica M, Lan L, Lorente G, Duan JX, Cai X, Mowday AM, Guise CP, et al. Molecular and cellular pharmacology of the hypoxia-activated prodrug TH-302. *Mol Cancer Ther* 2012; 11:740-51; PMID:22147748; <http://dx.doi.org/10.1158/1535-7163.MCT-11-0634>
 20. Sun JD, Liu Q, Wang J, Ahluwalia D, Ferraro D, Wang Y, Duan JX, Ammons WS, Curd JG, Matteucci MD, et al. Selective tumor hypoxia targeting by hypoxia-activated prodrug TH-302 inhibits tumor growth in preclinical models of cancer. *Clin Cancer Res* 2012; 18:758-70; PMID:22184053; <http://dx.doi.org/10.1158/1078-0432.CCR-11-1980>
 21. Liu Q, Sun JD, Wang J, Ahluwalia D, Baker AF, Cranmer LD, Ferraro D, Wang Y, Duan JX, Ammons WS, et al. TH-302, a hypoxia-activated prodrug with broad in vivo preclinical combination therapy efficacy: optimization of dosing regimens and schedules. *Cancer Chemother Pharmacol* 2012; 69:1487-98; PMID:22382881; <http://dx.doi.org/10.1007/s00280-012-1852-8>
 22. Jemal A, Siegel R, Ward E, Hao Y, Xu J, Murray T, Thun MJ. *Cancer Stat* 2008; 58:71-96; PMID:18287387
 23. Burris HA 3rd, Moore MJ, Andersen J, Green MR, Rothenberg ML, Modiano MR, Cripps MC, Portenoy RK, Storniolo AM, Tarassoff P, et al. Improvements in survival and clinical benefit with gemcitabine as first-line therapy for patients with advanced pancreas cancer: a randomized trial. *J Clin Oncol* 1997; 15:2403-13; PMID:9196156
 24. Moore MJ, Goldstein D, Hamm J, Figer A, Hecht JR, Gallinger S, Au HJ, Murawa P, Walde D, Wolff RA, et al. Erlotinib plus gemcitabine compared with gemcitabine alone in patients with advanced pancreatic cancer: a phase III trial of the National Cancer Institute of Canada Clinical Trials Group. *J Clin Oncol* 2007; 25:1960-6; PMID:17452677; <http://dx.doi.org/10.1200/JCO.2006.07.9525>
 25. Borad MJ, Reddy S, Uronis H, Sigal DS, Cohn AL, Schelman WR, Stephenson J, Chiorean EG, Rosen PJ, Ulrich B, et al. Randomized phase II study of the efficacy and safety of gemcitabine + TH-302 (G+T) vs gemcitabine (G) alone in previously untreated patients with advanced pancreatic cancer. *Cancer Res* 2012; 72 (Suppl 1); Abst. LB-121
 26. Sparreboom A, Scripture CD, Trieu V, Williams PJ, De T, Yang A, Beals B, Figg WD, Hawkins M, Desai N. Comparative preclinical and clinical pharmacokinetics of a cremophor-free, nanoparticle albumin-bound paclitaxel (ABI-007) and paclitaxel formulated in Cremophor (Taxol). *Clin Cancer Res* 2005; 11:4136-43; PMID:15930349; <http://dx.doi.org/10.1158/1078-0432.CCR-04-2291>
 27. Von Hoff DD, Ervin T, Arena FP, Chiorean EG, Infante J, Moore M, Seay T, Tjulandin SA, Ma WW, Saleh MN, et al. Increased survival in pancreatic cancer with nab-paclitaxel plus gemcitabine. *N Engl J Med* 2013; 369:1691-703.
 28. Alvarez R, Musteanu M, Garcia-Garcia E, Lopez-Casas PP, Megias D, Guerra C, Muñoz M, Quijano Y, Cubillo A, Rodriguez-Pascual J, et al. Stromal disrupting effects of nab-paclitaxel in pancreatic cancer. *Br J Cancer* 2013; 109:926-33; PMID:23907428; <http://dx.doi.org/10.1038/bjc.2013.415>
 29. Awasthi N, Zhang C, Schwarz AM, Hinz S, Wang C, Williams NS, Schwarz MA, Schwarz RE. Comparative benefits of Nab-paclitaxel over gemcitabine or polysorbate-based docetaxel in experimental pancreatic cancer. *Carcinogenesis* 2013; 34:2361-9; PMID:23803690; <http://dx.doi.org/10.1093/carcin/bgt227>
 30. Weiss GJ, Infante JR, Chiorean EG, Borad MJ, Bendell JC, Molina JR, Tibes R, Ramanathan RK, Lewandowski K, Jones SF, et al. Phase I study of the safety, tolerability, and pharmacokinetics of TH-302, a hypoxia-activated prodrug, in patients with advanced solid malignancies. *Clin Cancer Res* 2011; 17:2997-3004; PMID:21415214; <http://dx.doi.org/10.1158/1078-0432.CCR-10-3425>
 31. Jung D, Lin L, Jiao H, Cai X, Duan JX, Matteucci M. Pharmacokinetics of TH-302: a hypoxically activated prodrug of bromo-isophosphoramidate mustard in mice, rats, dogs and monkeys. *Cancer Chemother Pharmacol* 2012; 69:643-54; PMID:21964906; <http://dx.doi.org/10.1007/s00280-011-1741-6>
 32. Chu GC, Kimmelman AC, Hezel AF, DePinho RA. Stromal biology of pancreatic cancer. *J Cell Biochem* 2007; 101:887-907; PMID:17266048; <http://dx.doi.org/10.1002/jcb.21209>
 33. Mahadevan D, Von Hoff DD. Tumor-stroma interactions in pancreatic ductal adenocarcinoma. *Mol Cancer Ther* 2007; 6:1186-97; PMID:17406031; <http://dx.doi.org/10.1158/1535-7163.MCT-06-0686>
 34. Hidalgo M, Von Hoff DD. Translational therapeutic opportunities in ductal adenocarcinoma of the pancreas. *Clin Cancer Res* 2012; 18:4249-56; PMID:22896691; <http://dx.doi.org/10.1158/1078-0432.CCR-12-1327>
 35. Kallman RF, Dorie MJ. Tumor oxygenation and reoxygenation during radiation therapy: their importance in predicting tumor response. *Int J Radiat Oncol Biol Phys* 1986; 12:681-5; PMID:3700172; [http://dx.doi.org/10.1016/0360-3016\(86\)90080-5](http://dx.doi.org/10.1016/0360-3016(86)90080-5)
 36. Dorie MJ, Kallman RF. Reoxygenation in the RIF-1 tumor after chemotherapy. *Int J Radiat Oncol Biol Phys* 1992; 24:295-9; PMID:1382047; [http://dx.doi.org/10.1016/0360-3016\(92\)90684-A](http://dx.doi.org/10.1016/0360-3016(92)90684-A)
 37. Von Hoff DD, Ramanathan RK, Borad MJ, Laheru DA, Smith LS, Wood TE, Korn RL, Desai N, Trieu V, Iglesias JL, et al. Gemcitabine plus nab-paclitaxel is an active regimen in patients with advanced pancreatic cancer: a phase I/II trial. *J Clin Oncol* 2011; 29:4548-54; PMID:21969517; <http://dx.doi.org/10.1200/JCO.2011.36.5742>
 38. Ide T, Kitajima Y, Miyoshi A, Ohtsuka T, Mitsuno M, Ohtaka K, Miyazaki K. The hypoxic environment in tumor-stromal cells accelerates pancreatic cancer progression via the activation of paracrine hepatocyte growth factor/c-Met signaling. *Ann Surg Oncol* 2007; 14:2600-7; PMID:17534684; <http://dx.doi.org/10.1245/s10434-007-9435-3>
 39. Pizzi S, Porzionato A, Pasquali C, Guidolin D, Sperti C, Fogar P, Macchi V, De Caro R, Pedrazzoli S, Parenti A. Glucose transporter-1 expression and prognostic significance in pancreatic carcinogenesis. *Histol Histopathol* 2007; 24:175-8540.
 40. Soffietti R, Trevisan E, Rudà R. Neurologic complications of chemotherapy and other newer and experimental approaches. *Handb Clin Neurol* 2014; 121:1199-218; PMID:24365412
 41. Hureauux J, Lagarce F, Gagnadoux F, Rousselet MC, Moal V, Urban T, Benoit JP. Toxicological study and efficacy of blank and paclitaxel-loaded lipid nanocapsules after i.v. administration in mice. *Pharm Res* 2010; 27:421-30; PMID:20054705; <http://dx.doi.org/10.1007/s11095-009-0024-y>
 42. Houghton PJ, Morton CL, Tucker C, Payne D, Favours E, Cole C, Gorlick R, Kolb EA, Zhang W, Lock R, et al. The pediatric preclinical testing program: description of models and early testing results. *Pediatr Blood Cancer* 2007; 49:928-40; PMID:17066459; <http://dx.doi.org/10.1002/pbc.21078>
 43. Chaplan SR, Pogrel JW, Yaksh TL. Role of voltage-dependent calcium channel subtypes in experimental tactile allodynia. *J Pharmacol Exp Ther* 1994; 269:1117-23; PMID:8014856
 44. Porec LR, Guo TZ, Kingery WS, Maze M. The analgesic potency of dexmedetomidine is enhanced after nerve injury: a possible role for peripheral alpha2-adrenoceptors. *Anesth Analg* 1998; 87:941-8; PMID:9768799